J. Astrophys. Astr. (1995) **16,** 327–355

Polarization-Mode Separation and the Emission Geometry of Pulsar 0823 + 26: A New Pattern of Pulsar Emission?

Joanna M. Rankin *Physics Department, University of Vermont, Burlington, Vermont 05405 USA*

N. Rathnasree *Raman Research Institute, Bangalore 560 080 India*

Received 1995 August 29; accepted 1995 November 17

Abstract. We explore the detailed polarization behaviour of pulsar 0823 + 26 using the technique of constructing partial 'mode-separated' profiles corresponding to the primary and secondary polarization modes. The characteristics of the two polarization modes in this pulsar are particularly interesting, both because they are anything but orthogonal and because the secondary mode exhibits a structure seen neither in the primary mode nor in the total profile. The new leading and trailing features in the secondary mode, which appear to represent a conal component pair, are interpreted geometrically on the basis of their width and the associated polarization-angle traverse as an outer cone.

If the secondary-mode features are, indeed, an outer cone, then questions about the significance of the pulsar's postcursor component become more pressing. It seems that 0823 + 26 has a very nearly equatorial geometry, in that both magnetic poles and the sightline all fall close to the rotational equator of the star. We thus associate the postcursor component with emission along those bundles of field lines which are also equatorial and which continue to have a tangent in the direction of our sight line for a significant portion of the star's rotation cycle. It seems that in all pulsars with postcursor components, this emission follows the core component, and all may thus have equatorial emission geometries. No pulsars with precursors in this sense – including the Crab pulsar – are known.

The distribution of power between the primary and secondary modes is very similar at both 430 and 1400 MHz. Our analysis shows that in this pulsar considerable depolarization must be occurring on time scales that are short compared to the time resolution of our observations, which is here some 0.5–1.0 milliseconds. One of the most interesting features of the mode-separated partial profiles is a phase offset between the primary and secondary modes. The secondary-mode 'main pulse' arrives some 1.5 ± 0.1° before the primary-mode one at 430 MHz and some 1.3 ± 0.1° at 21 cm. Given that the polar cap has an angular diameter of 3.36°, we consider whether this is a geometric effect or an effect of differential propagation of the two modes in the inner magnetosphere of the pulsar.

Key words: Pulsars—polarization—PSR B0823 + 26.

1. Introduction

Pulsar B0823 + 26 is one of the oldest known pulsars, being the first or second pulsar discovered at the Arecibo Observatory (Craft, Lovelace & Sutton 1968). With a period of 531 ms and a spindown of 1.72×10^{-15} sec/sec – yielding a B_{12}/P^2 value of 3.44 – its timing properties could not be more ordinary. However, Backer *et al.* (1973) discovered that the pulsar has both an interpulse (IP) and a postcursor (PC) component. The pulsar is also relatively close (DM $\sim 19.5\,\mathrm{pc/cm^3}$), bright, and exhibits a turnover in its radio-frequency spectrum only below about 50 MHz (Sieber 1973; Izvekova *et al.* 1981). For all of these reasons, it has been possible to study it over a remarkably wide interval of frequency. On the high end it has been detected at Bonn by Bartel *et al.* (1978) at 14.8 GHz, and observations on the low end have been reported at 26 MHz (Phillips & Wolszczan 1992).

Over this enormous frequency range the form of the pulsar's profile changes remarkably little [see Hankins & Rickett (1986) for a series of profiles spanning 135 to 2380 MHz]. The MP exhibits a nearly Gaussian-shaped profile at both the very highest and lowest frequencies, only distorted by what is probably interstellar scattering at 26 MHz. Its width does change, however, from being practically constant above 1 GHz, to growing with an asymptotic dependence of about $f^{-0.58}$ below about 300 MHz (Rankin 1983b; hereafter Paper II). The half-power width of the MP, interpolated to 1 GHz, was determined in Rankin (1990; hereafter Paper IV) to be 3.38°, very close to the $2.45°/P^{1/2}$ angular diameter of the pulsar's polar cap at the surface of the star.

The MP-IP spacing is very close to 180° and could be independent of frequency, although a slight decrease with frequency is also compatible with the observations (Hankins & Fowler 1986). The MP-PC separation, however, *increases* monotonically with frequency between about 400 and 2400 MHz as $f^{0.08}$ (Hankins & Fowler 1986), and Arecibo 130-MHz observations further confirm this behaviour (Hankins & Rankin 1994). The relative intensity of the IP is strongest at 400 MHz, with a peak intensity of just under 1 per cent that of the MP, and decreases steadily at both higher and lower frequencies. The PC, in turn, is somewhat stronger than the IP, being about 3 per cent of the MP at 400 MHz. At frequencies above about 400 MHz the relative intensities of the PC and IP fall off at about the same rate ($f^{\sim -1}$). Below 400 MHz, the relative intensity of the IP decreases very rapidly, whereas that of the PC increases, at least to about 100 MHz, though far less steeply than at higher frequencies (Hankins & Rankin 1994).

Full period, average polarimetry has been published for pulsar 0823 + 26 at 430 MHz (Rankin & Benson 1981), 1400 MHz (Rankin *et al.* 1989; Blaskiewicz *et al.* 1991), and 10.55 GHz (Xilouris *et al.* 1995), all but the last of which also includes some information about the PC and/or the IP. Individual-pulse polarimetric studies have been carried out at 430 MHz (Rankin *et al.* 1974; Backer & Rankin 1980) and 1400 MHz (Stinebring *et al.* 1984). The aggregate linear polarization is also Gaussian in form, occupies the central portion of the profile, and is never large—going from perhaps 35% at 430 MHz, to 25% at 1400 MHz, and 5% at 10.55 GHz. The edges of the profile are thus almost completely depolarized, but slightly more so on the leading than the trailing edge so that the residual linear 'component' looks a little delayed relative to the total-power profile.

A small amount of circular polarization is also observed in this pulsar's average profile, usually less than 5%. The published profiles often show a little left-hand (positive) circular on the leading edge, changing to a little more right-hand (negative) on the trailing. However, other unpublished observations suggest considerable variation around this general configuration.

With not only an MP, but an IP and PC as well, the linear polarization angle (PA) can be measured over a large part of the star's rotation cycle. Backer & Rankin (1980), however, found the linear PA behaviour of this pulsar to be unusually complex, apparently requiring two different angle systems. Using the information in Rankin & Benson (and correcting for '90° flips' at about -8 and $+12°$), Lyne & Manchester (1988) have obtained a value of 80° for α, the angle between the magnetic and rotation axes of the star, by fitting the single-vector model (Radhakrishnan & Cooke 1969; Komesaroff 1970) to the PA data. Better resolved observations are to be found in Rankin *et al.* (1989) and Blaskiewicz *et al.* (1991), and the rapid traverse of the PA near the peak of the profile can be seen clearly. The latter study (also correcting for a '90° flip' at about 170° in the 430-MHz observation) obtained values of $79° \pm 1°$ and $91° \pm 600°$ at 430 and 1418 MHz, respectively.

Fluctuation-spectral analysis yields a 'weak, broad feature in the range of 0.05 to $0.23c/P_1$ with a constant strength of 0.35..... The measured center frequency is $0.14c/P_1$' (Backer 1973). In other studies (Taylor & Huguenin 1969; Lang 1969), the feature appeared stronger and at a frequency of 0.18 to $0.20c/P_1$. We note here [and Rankin (1986; hereafter Paper III) did not!] that there is considerable fluctuation power at frequencies below $0.10c/P_1$, suggesting in the terms of Paper III both core and conal-associated fluctuations. Finally, there is no published evidence for null pulses, although the limit of $\leqslant 5\%$ (Ritchings 1976) is not a very strong one.

As regards classification, pulsar 0823 + 26 has had a chequered history. In Paper III it was seen as a conal double (D) pulsar in an attempt to make sense of the MP and PC as a conal component pair. The spacing between the two components was uncomfortably large, and there was some antisymmetric MP circular polarization, but the lack of MP conal 'outriders' at high frequency tilted toward the conal side. The growing weight of evidence regarding core-component geometry in Paper IV shifted 0823 + 26 into the core-single (S_t) class. Its MP width was exactly what would be expected for a core component in a pulsar with a nearly orthogonal magnetic geometry, a geometry which seemed highly compatible with its observed interpulse. Its rather high B_{12}/P^2 also seemed to suggest that it is not a cone-dominated pulsar. And viewing the MP as primarily a core component was more compatible with its polarization characteristics. This classification left only two nagging questions: **a)** In a pulsar which can be observed to such high frequencies, where are the high frequency conal 'outriders'? And **b)** If the MP is a core component, how are we now to interpret the PC?

These questions are the starting point for this paper. In the next section we introduce the observations considered in our analysis, and §3 begins our discussion of the polarization structure of pulsar 0823 + 26's profile. In §4 we consider mode-separation techniques and their application to pulsar 0823 + 26, §5–§7 explore the pulsar's main-pulse, postcursor, and interpulse emission geometry, respectively, §8 then returns to the polarization-modal structure of the main-pulse emission, §9 assesses the significance of the displaced modal emission, and §10 provides a summary and the conclusions of the paper.

2. Observations

The single-pulse observations used in our analysis below come from three programs carried out at the Arecibo Observatory over a long period of time. The older 430-MHz

observations were carried out in January 1974 with a single-channel adding polarimeter of 500-kHz bandwidth and 1.0-ms integration time, giving a nominal time resolution of about 0.7° longitude. The polarimetry scheme is described in Rankin *et al.* (1975); no attempt was made to correct the Stokes parameters for the known 0.25% cross-coupling in the feed, which can produce spurious circular polarization at a nominal level of about 10% of the linear.

The older 1400-MHz observations were carried out in October 1981, again with a single-channel, adding polarimeter. Here the bandwidth was 10 MHz and time constant 0.66 ms, giving an effective resolution of about 0.5°. A serious effort was made for the first time to correct the measured Stokes parameters for instrumental distortion using the 'orthogonal' approximation described by Stinebring *et al.* (1984).

The newer observations at 430 and 1404 MHz were made in a single observing session in October 1992, the 430 MHz on the morning of the 20th and the 21 cm on the morning of the 15th. Both used a special program to gate the 40-MHz correlator, and the basic data recorded at the telescope were the ACFs and CCFs of the right- and left-hand channel voltages. The higher frequency observations used a 20-MHz BW and the lower a 10-MHz BW, and the retention of 32 lags in both cases reduced dispersion delay across the bandpass to negligible levels. The resolution was then essentially the correlator dump time, which was 506 μs or 0.34°. The Arecibo 40-MHz correlator is described by Hagan (1987) and the observing software by Perillat (1988, 1992). The measured correlation functions were scaled, 3-level sampling corrected, and Fourier transformed to produce raw Stokes parameters, which were in turn corrected (channel by channel) for dispersion, Faraday rotation, instrumental delays, and all of the known feed imperfections as determined by full-sky tracks of pulsar 1929 + 10 and other sources. During the course of our analysis, we discovered that the instrumental polarization is highly frequency dependent, particularly at 430 MHz; therefore, the most recent observations represent some of the best calibrated ever made at the Arecibo Observatory. The instrumental details will be described in a forthcoming paper (Rankin, Rathnasree & Xilouris 1996).

3. The polarization structure of pulsar 0823 + 26's profile

Figures 1a–c give a collection of profile and polarization-angle density plots for both 430 and 1404 MHz. Notice the difference in the longitude scales; at 430 MHz the entire MP-PC portion of the rotation cycle of the pulsar is included, whereas at 1404 MHz only the MP region is plotted. We should say that the lower panels are not really grey-scale plots; each point represents the polarization of an actual measured sample falling above a threshold of a few standard deviations in the off-pulse noise. The regions of greatest primary-mode power are thus 'over exposed' in the process of plotting enough individual pulses to explore the overall space represented by the diagram.

These plots are interesting and remarkably complex. Let us first consider the simpler 1404-MHz diagram (Fig. 1c), wherein it is clear that there are two distinct modes and that these have very different PA traverses. One can also see this, both in Stinebring *et al.*'s Fig. 5 and in Gil *et al.*'s Fig. 2 – we are dealing here with the same data – but considerably less clearly owing to the details of plotting or analysis. The darker primary mode has a slope of 14–15°/°, and the less prominent secondary mode a slope just about twice this. What is most striking is that the two modes are anything but orthogonal, and

near the trailing edge of the profile (near + 3° longitude) appear to be separated by barely 45°. Lest anyone wish to attribute this to instrumental causes, we have another, shorter 1404-MHz sequence from our 1992 October observations which shows an identical behaviour. Other than this it is interesting to again note the minor peak in the linear power as well as the larger one, which trails the profile center. Also one can see, both how narrow the longitude interval over which the PA can be traced is and how poorly it often traces the PA of the primary-mode power.

We see a good deal more in the 430-MHz figures (Figs. 1a and b), and it is noteworthy how much more similar the PA density plots are than the average position-angle behaviour. The primary and secondary modes are again prominent in the center of the profile, and their measured slopes are nearly the same as at 21 cm.

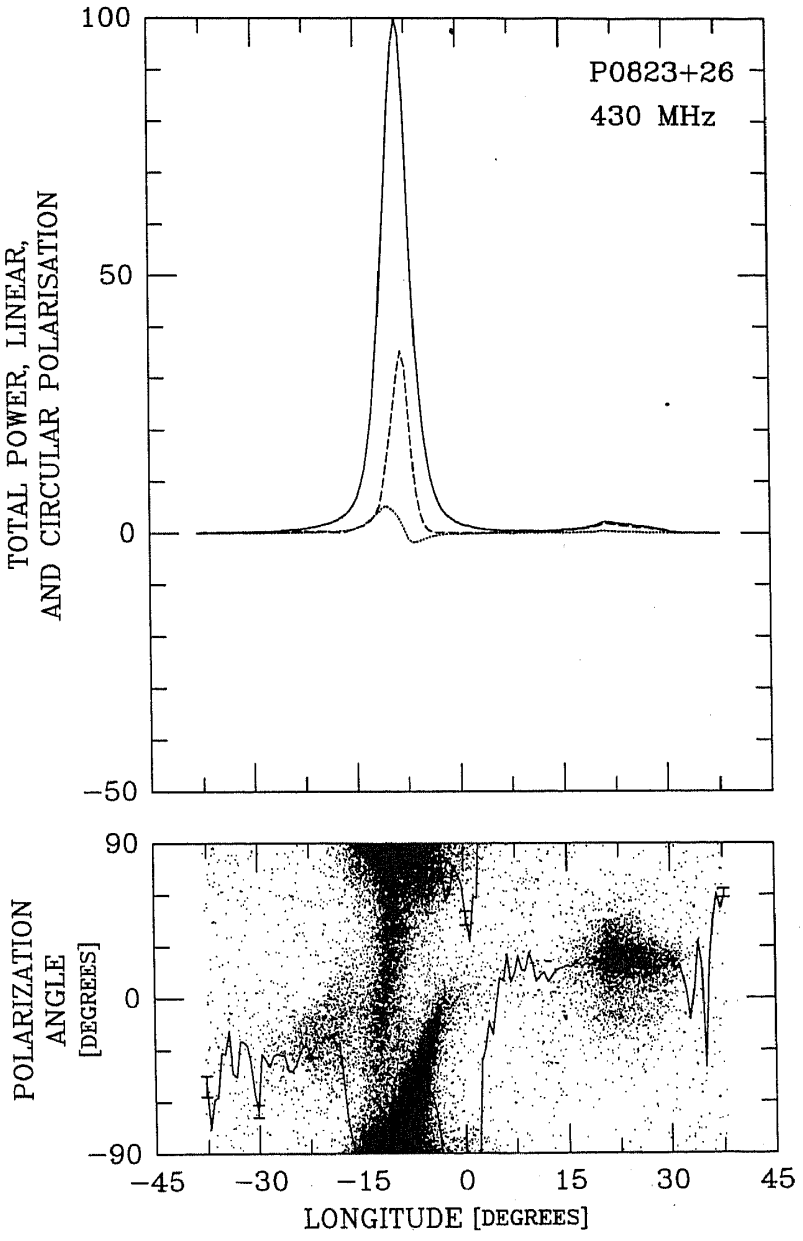

Figure 1(a).

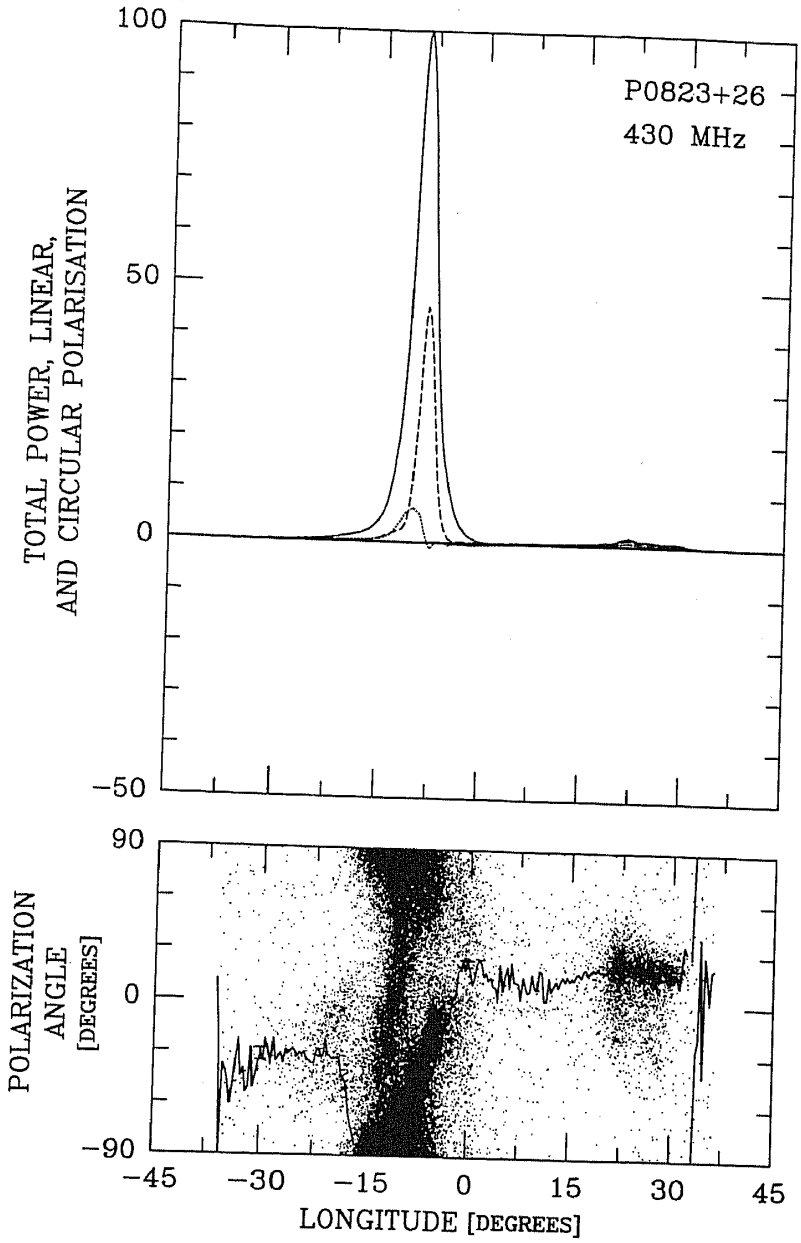

Figure 1(b).

Again there is rather little aggregate linearly polarized power outside the MP center, but owing to the greater intensity of the pulsar at 430 MHz, individual samples with sufficient power to define the PA can be found over nearly a quarter of the rotation cycle of the pulsar. The principal primary-mode 'blotch' begins at about $-12°$ longitude and $\pm 90°$ PA and rotates positively through about 90°, also making the largest contribution to the overall linearly polarized power, *L*. Several other 'patches' of significant linear polarization can also be seen: Note the area associated with the postcursor, another on the extreme leading edge of the profile (which can also be seen in *L*), and a third, secondary-mode 'blotch' which begins at about $-14°$ longitude and $-45°$ PA, again rotating positively through 90°. At this point this last traverse appears to flatten off adjacent to the principle primary-mode 'blotch', and its power is conflated with the main primary-mode 'blotch' in *L*.

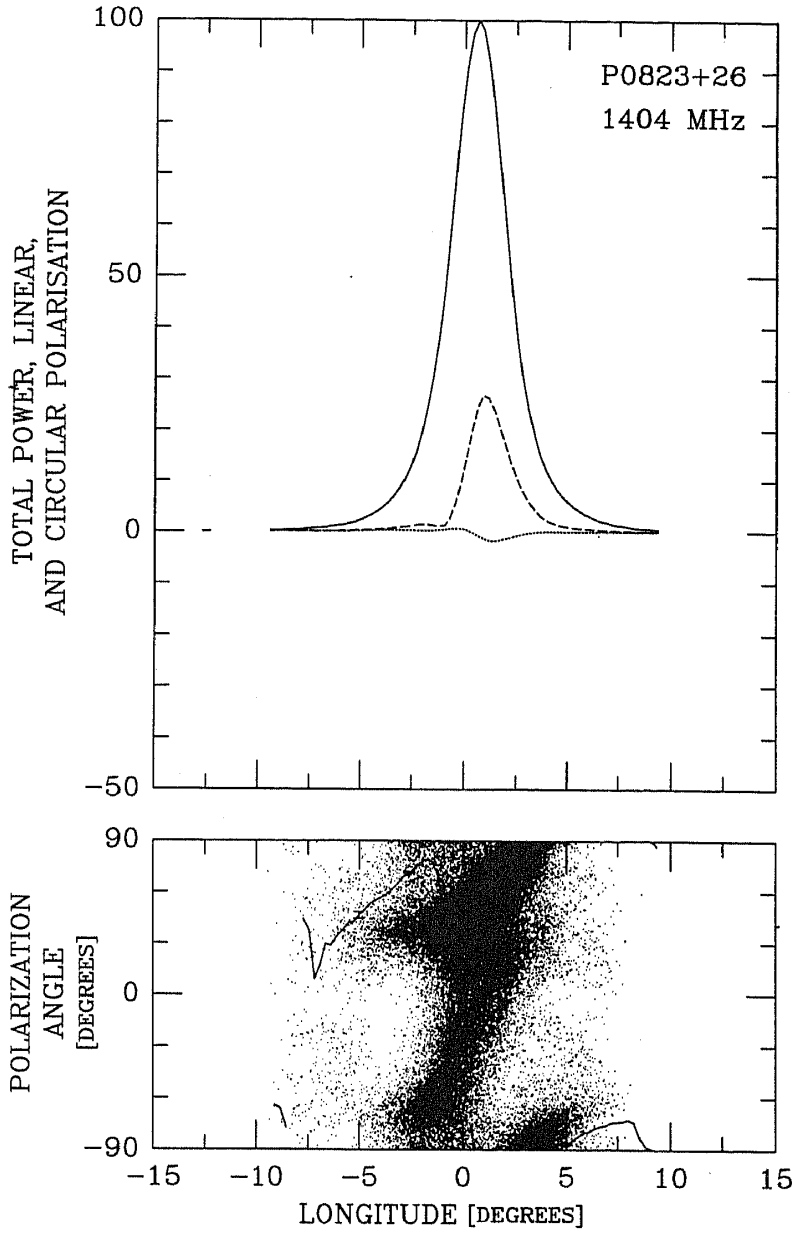

Figure 1(c).

Figure 1(a–c). Average profiles and polarization-angle density plots for pulsar 0823 + 26 at 430 MHz (**a**, **b**), and 1404 MHz (**c**). The upper panel plots Stokes parameter I, the total power (solid curve), $L = (Q^2 + U^2)^{1/2}$, the total linear polarization (dashed curve), and V, the circular polarization (dotted curve). The lower panel gives the polarization position angle of each sample falling above some threshold (see text), and the average position angle is also plotted, where defined, as a solid curve. The 430-MHz observations were recorded on 6th January 1974 and 20th October 1992 and represent 3194 and 1800 pulses, respectively. The 1404-MHz observation was made on 9th October 1982 and represents 6200 pulses.

Again it is interesting to consider how different the overall linear PA traverse is in the two 430-MHz observations, given the striking similarity of their modal-power distributions. It does appear that the polarization of this pulsar shows significant time variability; the differences in fractional linear polarization, PA traverse, and the entirely different form of the circular are quite typical of other (not shown) observations in our

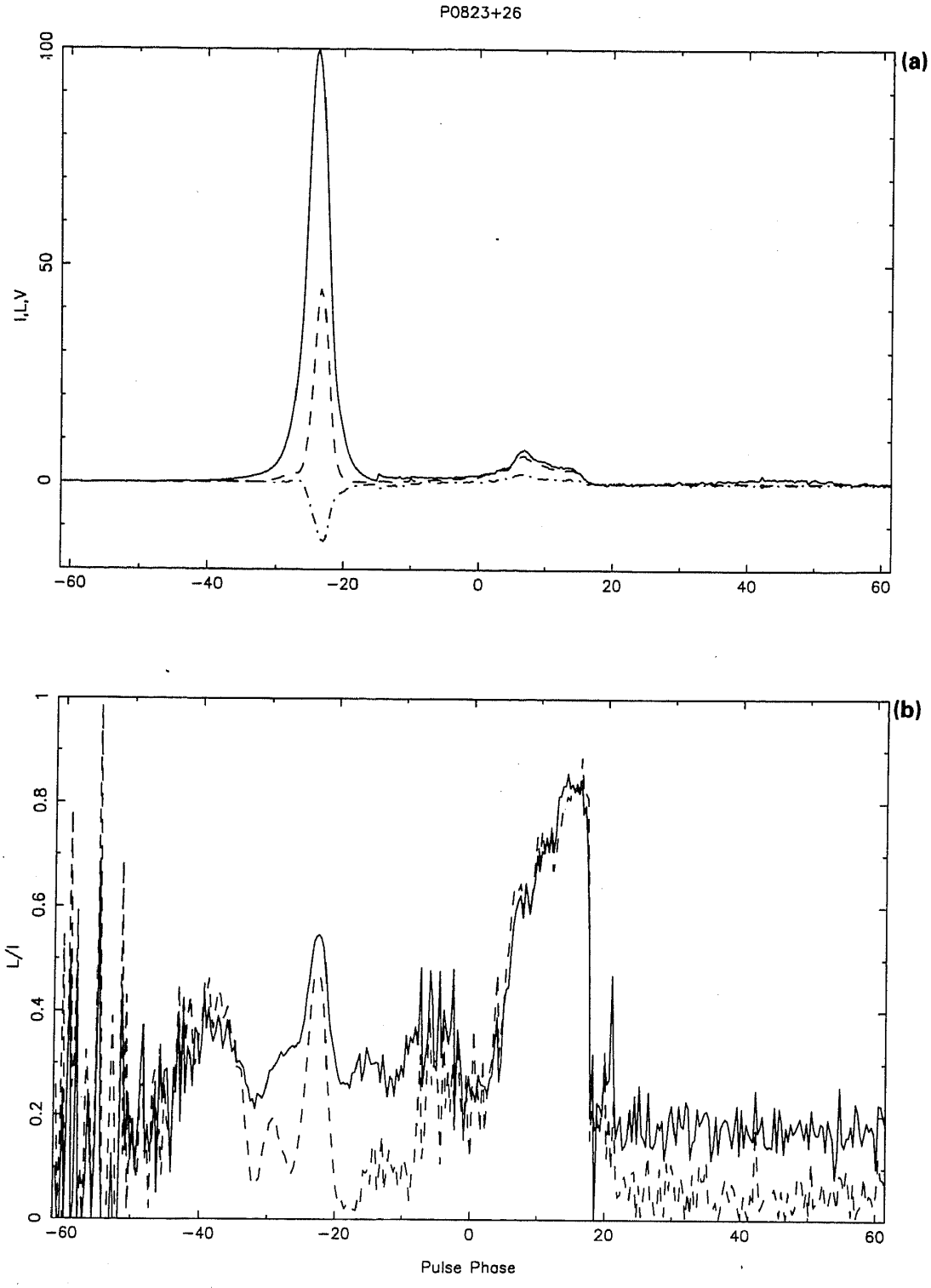

Figure 2. (**a**) Average profile of pulsar 0823 + 26 at 430 MHz as in Fig. 1b. At longitudes larger than − 15° all the quantities I, L and V have been multiplied by a factor of 5 to show the region of the postcursor more clearly. (**b**) The fractional linear polarization, $\langle L/I \rangle$ (solid curve) and $\langle L \rangle / \langle I \rangle$ (dashed curve). In both the curves the averages have been corrected for statistical polarization. In regions of low intensity, the degree of polarization could be quite undefined and oscillating between high and low values as in the left hand portion of the figure.

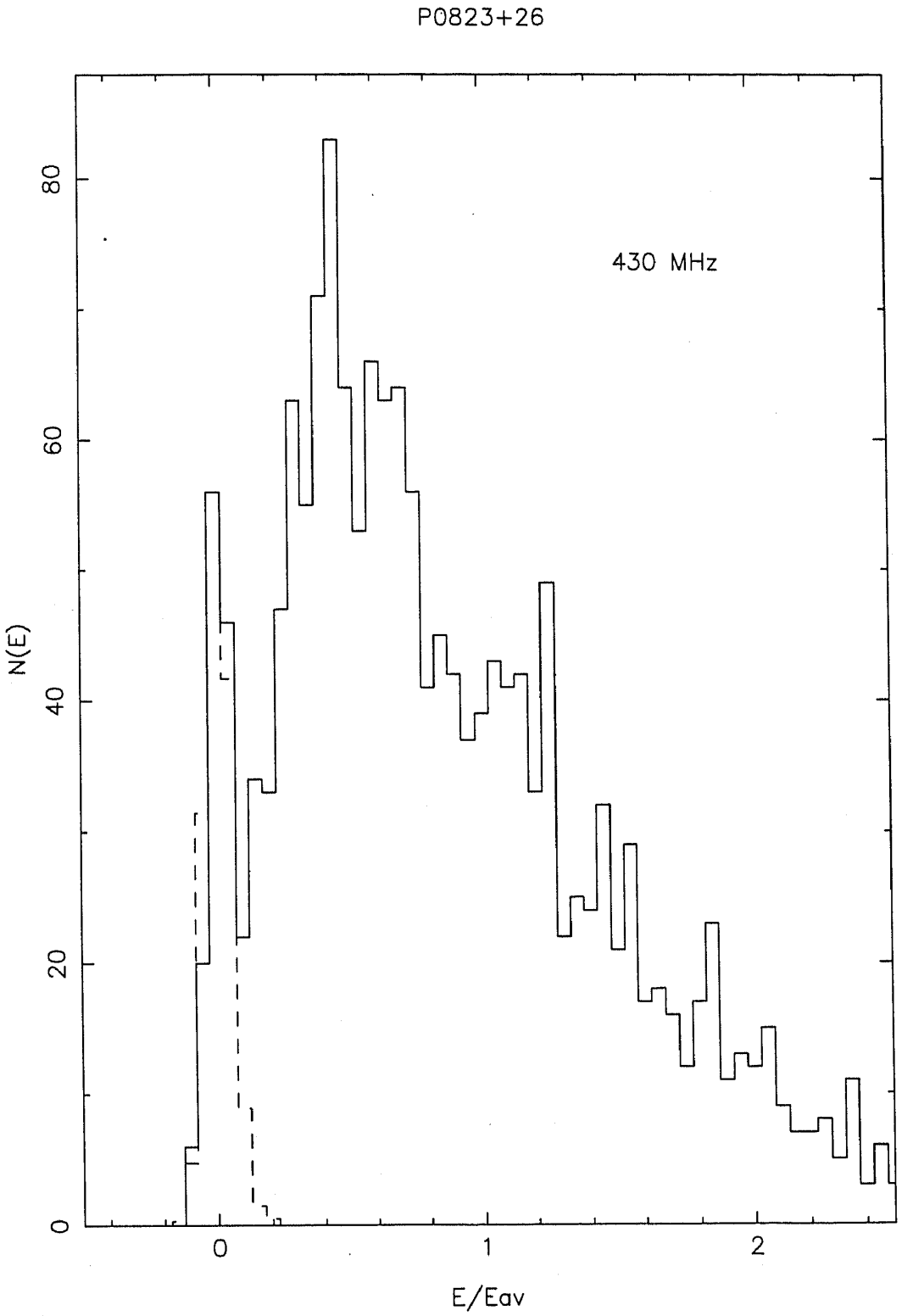

Figure 3. Pulse intensity histogram (solid line) for pulsar 0823 + 26 at 430 MHz corresponding to the October 1992 observations in Fig. 1b. The dashed line shows the intensity histogram obtained from the noise window, which is normalized to 142 pulses.

possession. It is quite conceivable that this pulsar exhibits some yet unrecognized mode-switching phenomenon (and of course this would be particularly difficult to identify in a pulsar with a single profile).

Turning now to Fig. 2, we again see the 430-MHz profile although displayed in a slightly different manner than in Fig. 1b. In the top panel, at all longitudes later than $-15°$, I, L and V have been multiplied by a factor of 5, so that the postcursor and interpulse windows can be seen more clearly. The information in the bottom panel has been obtained after rejecting sample by sample all data points with $I <$ twice the σ in the noise window. Here, we plot the fractional linear polarization, first in the usual manner by averaging Stokes parameters Q and U (dashed curve) and, second, by aggregating the linearly polarized power irrespective of the PA (solid curve). Under the MP peak the latter is larger than the former as expected, but generally only by some 10% or so, arguing that most of the depolarization is occurring on time scales short compared to the 500-μs resolution of the observation. However, the amount of depolarization taking place over time-scales larger than a period (which amounts to the difference between the two curves in the bottom panel) is considerably greater in the wings of the MP profile. This suggests that different processes and time scales of depolarization are operative in the MP wings, and overall, that the MP has a composite character. We will return to this issue below. Finally, note that exactly the opposite is true for the PC; the two linear polarization measures are identical within the noise, indicating that virtually no depolarization is occurring on time scales shorter than the sampling interval.

Finally, Fig. 3 gives a 430-MHz, pulse-intensity histogram, scaled to the average-profile intensity to show the range of fluctuation (solid line). A similar histogram (dashed line) for the noise window has been normalized so that the zero-intensity bins coincide. Interestingly, the pulse-intensity histogram is bi-modal, and the distinct zero-energy peak has a width almost exactly equal to that of the noise distribution. The fraction of null pulses from this analysis is 6.4 ± 0.8% as compared with the upper limit of 5% from Ritchings' (1976) study.

4. Polarization-mode separation

Several efforts have been made to separate the polarization modes and to reconstruct the two modal pulse profiles. Cordes *et al.* (1978) first carried out this analysis for PSR $2020+28$, and Rankin *et al.* (1988) and Rankin (1988) then applied it to pulsars $1737+13$ and 1604–00, respectively. About this time Gil *et al.* (1991) developed a different polarization-mode fitting technique and applied it first to $0823+26$ observations at 1404 MHz and then to observations of a small group of other pulsars at the same frequency (Gil *et al.* 1992). The first technique relies on a model of the polarization angle as a function of longitude, usually the 'single-vector' model given by Radhakrishnan & Cooke (1969) and extended by Komesaroff (1970), whereas the second uses an algorithm which partitions the aggregate polarization angles into two groups statistically, longitude by longitude.

The two techniques are complementary in that, both have their strengths and weaknesses. The first technique is more sensitive and 'stable', but risks giving the false appearance that the modal PAs follow the model in regions of longitude where the modal power is negligible. Gil's technique, on the other hand, has the advantage of

being model-independent, but requires significant power in both modes at each longitude and easily loses track of the identity of the modes when they are discontinuous. Our study of 0823 + 26 uses only the first technique, because we were unable to obtain sensible results using Gil's technique on the 430-MHz observations.

The question then immediately arises regarding how this overall polarization PA behaviour should be interpreted. At 430 MHz, beginning with the primary mode, we see a positive, about 120° rotation of the PA which seems to terminate at around the PA of the PC; by this interpretation, however, there is no appreciable primary-mode power at longitudes earlier than that of the primary-mode 'blob'—a circumstance which is also largely true, we note, at 21 cm. What power there is at earlier longitudes is reasonably associated with the secondary mode, although the leading-edge patch seems somewhat disconnected from the main area where the secondary mode rotates

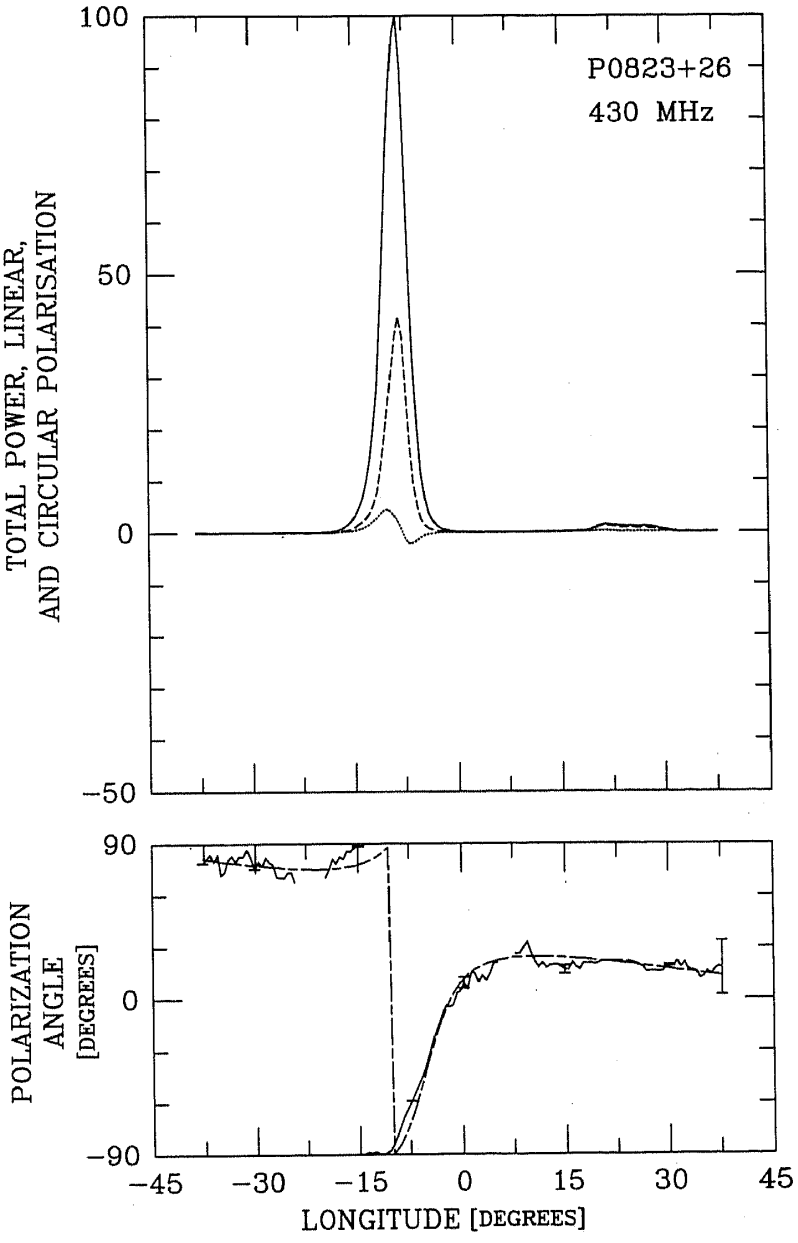

Figure 4(a).

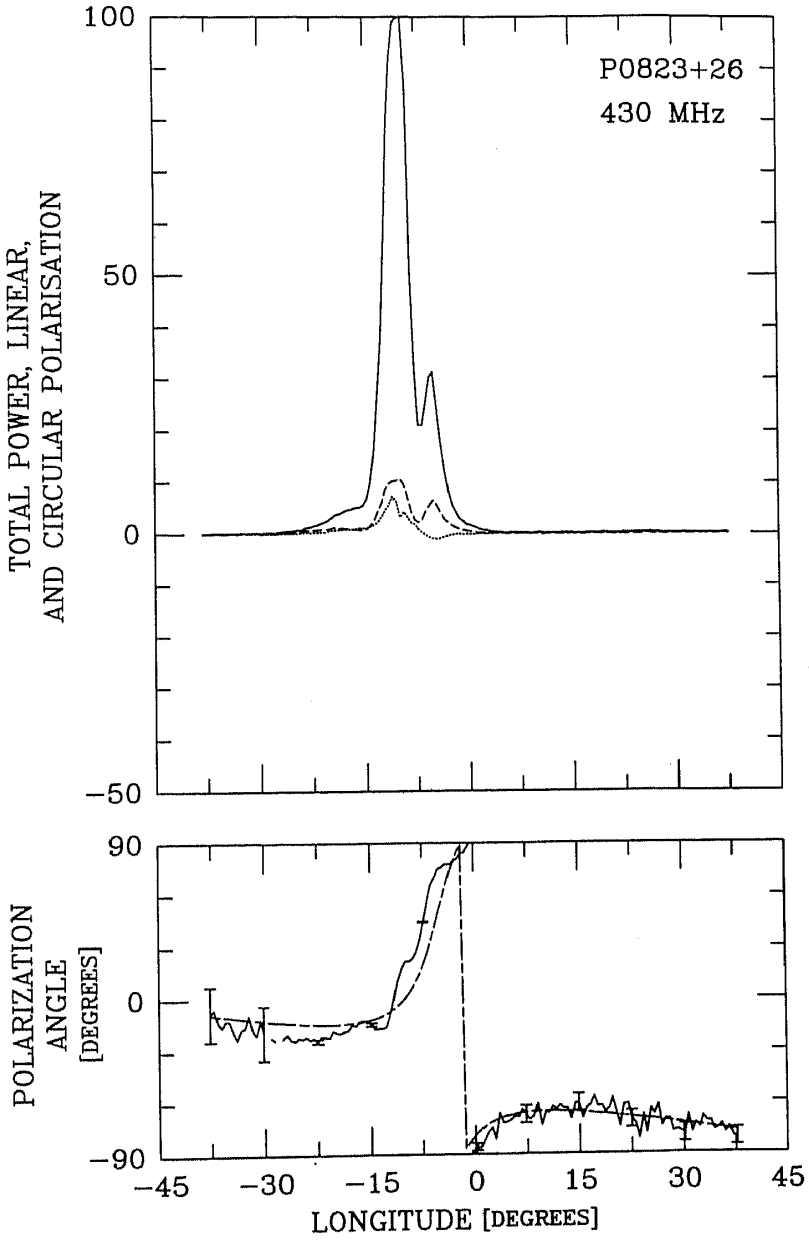

Figure 4(b).

most rapidly. It furthermore seems that the primary and secondary mode power
barely distinguishable in the 'patch' near -5 to $-10°$ longitude and $+75°$ I
Conveniently – despite the uncorrected ionospheric Faraday rotation – both 4
MHz observations have nearly the same PA origin.

Using this interpretation of the polarization-mode behaviour, we can begin
separate the composite profiles into their constituent polarization-modal par
profiles. In Rankin *et al.* (1988) we found a convenient representation of the sing
vector model

$$\chi = \chi_0 + \tan^{-1}\frac{\sin(\phi-\phi_0)}{A-\left(A-\frac{1}{R}\right)\cos(\phi-\phi_0)},$$

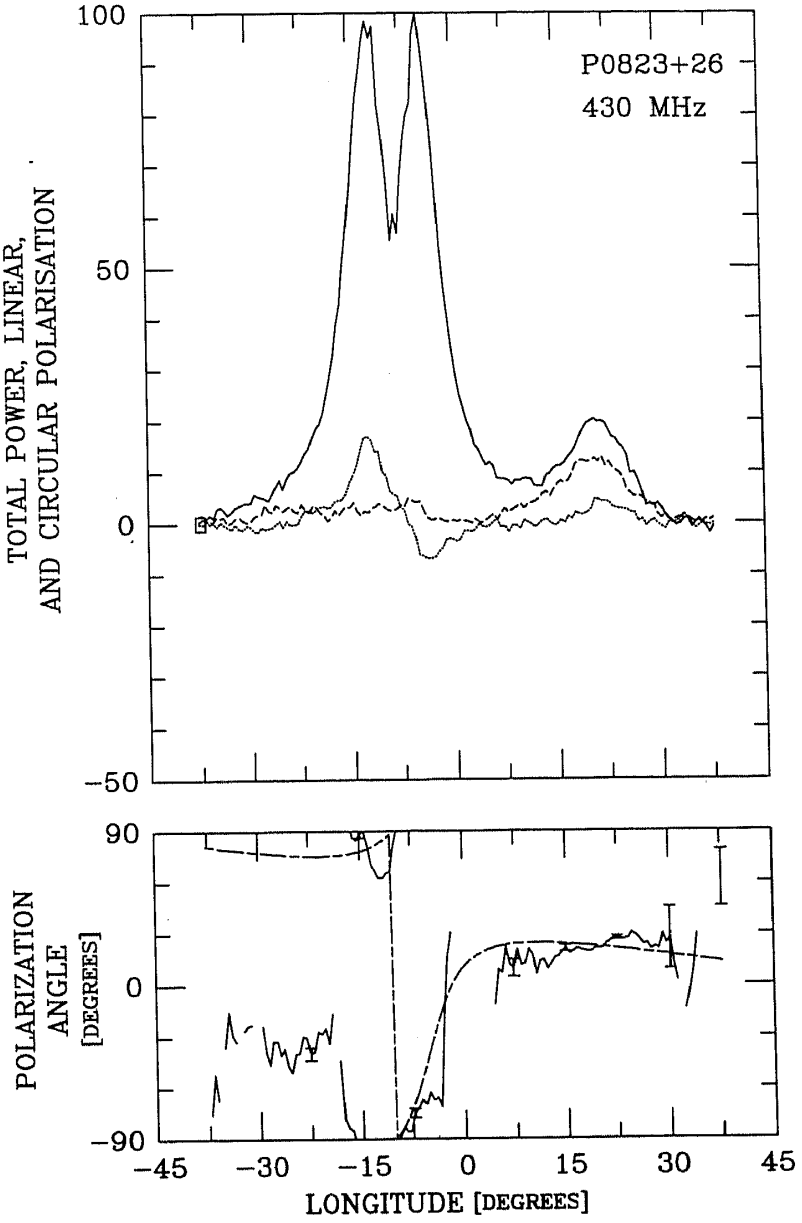

Figure 4(c).

Figure 4(a–c). Partial, 'mode-separated' profiles for pulsar 0823 + 26 at 430-MHz on 6th January 1974, (**a**) primary-mode, (**b**) secondary-mode, and (**c**) residual profiles. The lower panels in these figures give the PA traverses corresponding to the two modes, and the model PA is overplotted as a dashed curve.

where χ is the polarization angle, ϕ the longitude, $R = \left|\frac{d\chi}{d\phi}\right|_{max} = \sin\alpha/\sin\beta$ the maximum PA rate, and A a constant which can be computed from the total PA traverse χ_c between reference longitudes $\pm\phi_c$ as

$$A = \frac{\sin\phi_c/\tan\frac{1}{2}\chi_c - \cos\phi_c/|R|}{1-\cos\phi_c}$$

and which is formally equal to $\sin\zeta/\tan\alpha$, where α and ζ are the angles that the magnetic axis and the sight line make with the rotation axis, respectively.

Now taking the center of the primary-mode PA traverse at about $-4°$ longitude a PA of $-40°$, R as about $+15°/°$, and computing A from a total traverse χ_c of 12($\pm 30°$ longitude, we proceed to construct partial ('mode-separated') profiles cc sponding to the primary and secondary modes of 0823 + 26. The stream of sampl the individual pulses is compared with a threshold – the criteria being **a)** whether total linear polarization exceeds twice the off-pulse baseline noise level, and **b)** whe the computed PA falls within $\pm 45°$ of the model PA – and accumulated in one of tl partial profile 'bins' accordingly. The first, 'primary-mode' partial profile, consist those samples which both exceeded the noise threshold and had PAs lying on that of the Poincaré sphere closest to the Stokes vector representing the model PA, second those in the other hemisphere, and the third those which did not meet the n

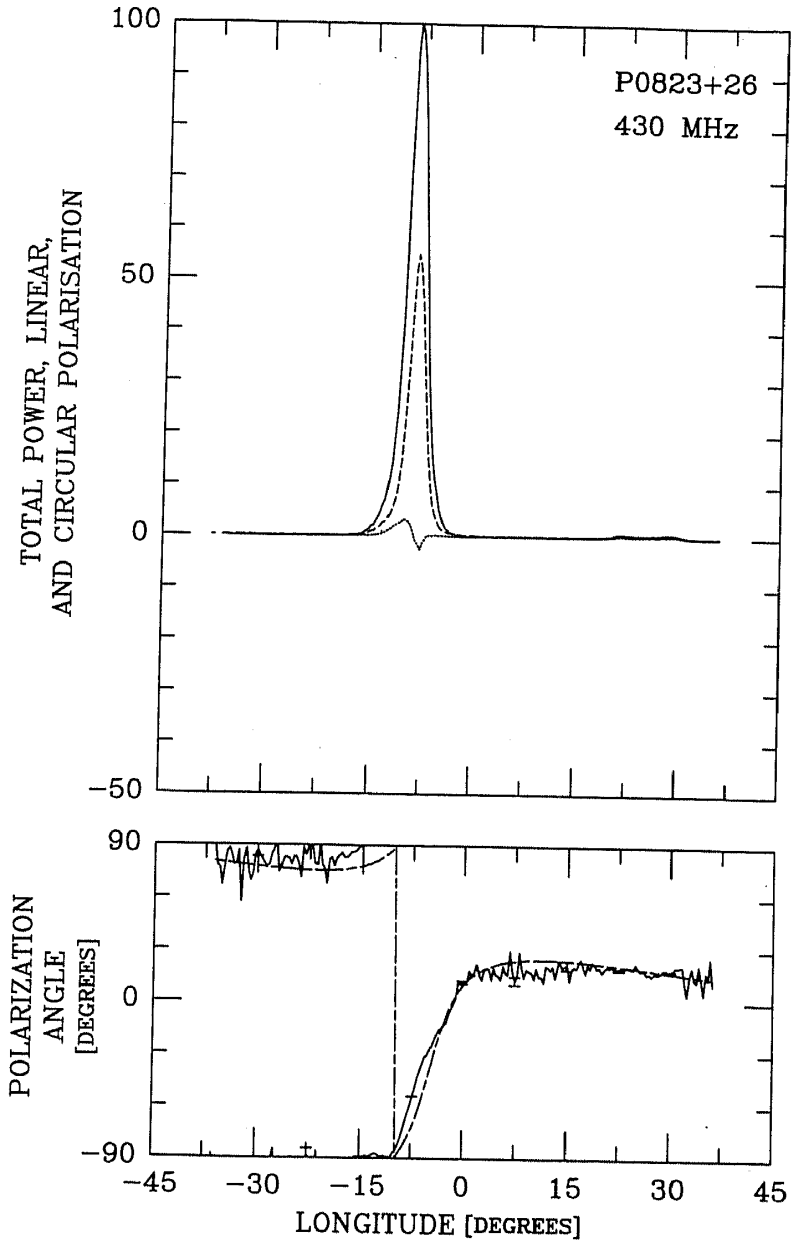

Figure 5(a).

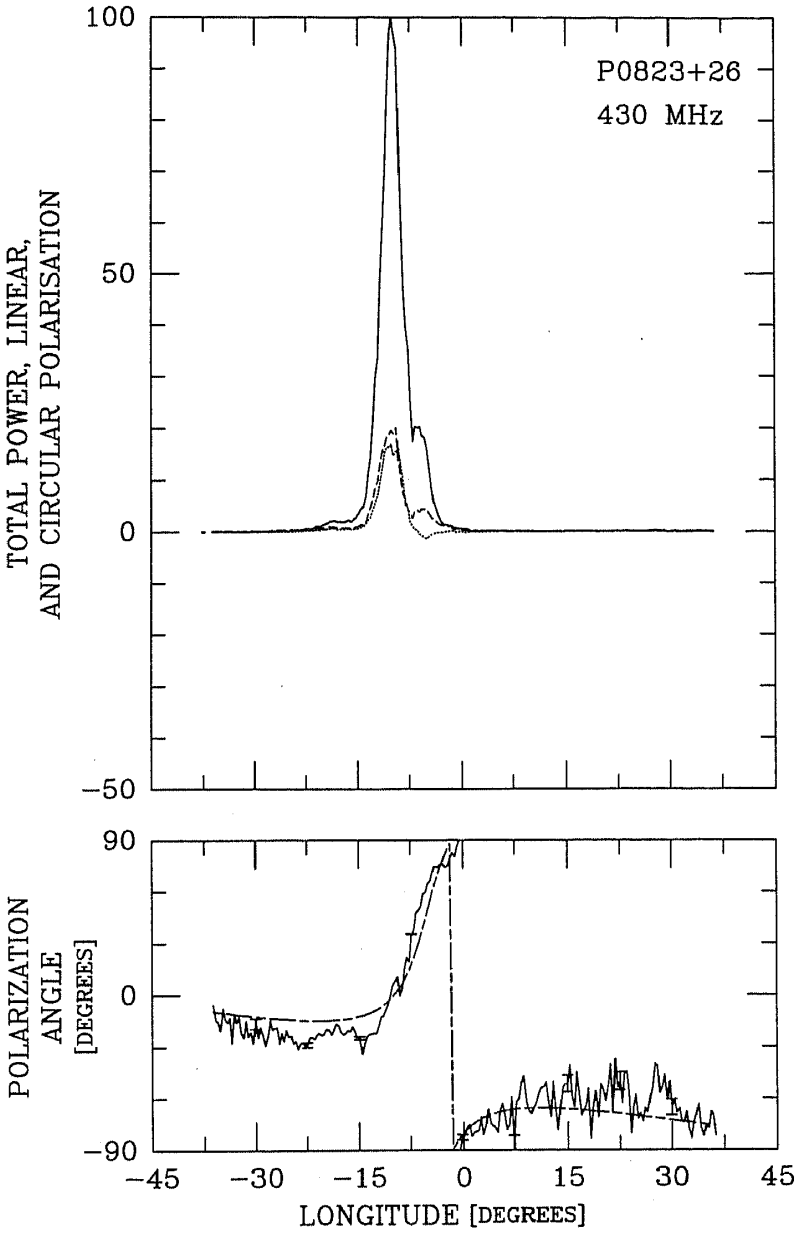

Figure 5(b).

threshold. The 'mode-separated' profiles at 430 MHz computed from the earlier 1974 and the later 1992 observations are given in Figs. 4 and 5, respectively.

Turning first to the earlier observations in Fig. 4, we see that the primary-mode partial profile (Fig. 4a) greatly resembles the total profile in Fig. 1a. The linear polarization is only a little greater, the circular polarization almost identical, only we now have an MP which is slightly narrower with its linear polarization more symmetrically positioned in its center. With a noise threshold of about 2-$\sigma^{\dagger}$ only about 9.9% of

[†]The precise off-pulse noise level is difficult to determine in the older observations as the noise-window data is no longer readily available; comparison with the 1992 observations – where the noise levels were accurately determined – however, shows that our estimate of σ is not far in error.

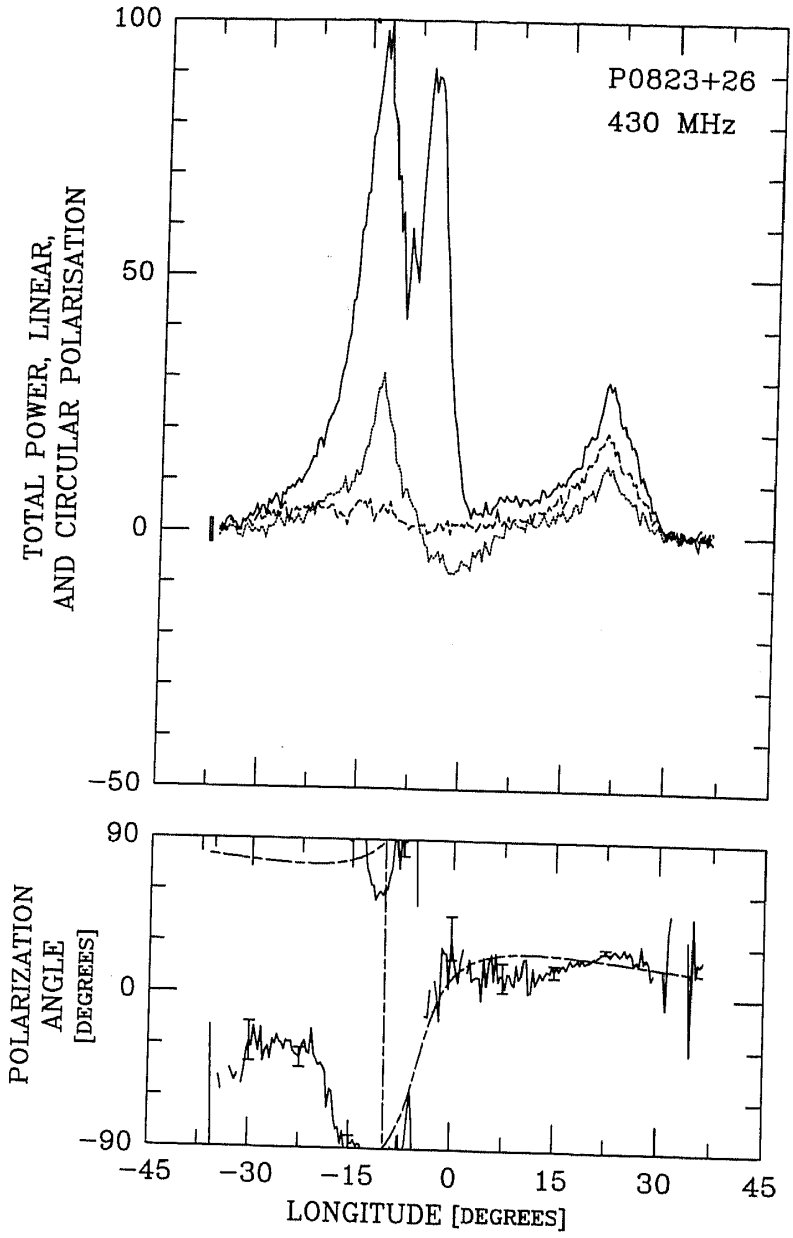

Figure 5(c).

Figure 5(a–c). Partial, 'mode-separated' profiles for pulsar 0823 + 26 at 430-MHz on 20th October 1992 as in Fig. 4.

the samples accrue to the primary-mode partial profile, but these carry nearly 67.9% of the total power. The only big change is in the PA traverse, which now more nearly conforms to what is expected on the basis of the single-vector model. Part of this is an artefact of the 'mode-separation' procedure; in regions of longitude where primary-mode L is small compared to the noise level – such as the 'baseline' region on the MP – the precise value of the model PA does affect the PA of the modal partial profile. However, in regions where any significant linear power is present, the partial profile PAs are only very weakly dependent upon the PA model. We also note that the PC is most prominent in the primary mode, and its linear polarization appears more complete because weakly polarized samples have not reached the noise threshold level.

It is the secondary-mode profile in Fig. 4b which holds the surprises, though it consists of only 4.1% of the samples and 17.7% of the power. This profile shows a more complex structure, both in L and in total power. Were it a complete profile, we would immediately say it had a triple form. The polarization is low, but not insignificant, throughout its entire extent; here we see much less severely depolarized 'wings' as compared with the primary-mode profile. Part of this is again an artefact of the separation in that, weakly polarized samples in the wings will have a much reduced chance of meeting the threshold in L; however, as we shall see below, this is not the whole story. Again, the PA traverse is 'rationalized', but it is also well defined over most of its extent by 'patches' of modal power. Note that here we see a flattening of the steep traverse after about $-15°$ longitude as compared to the density plot in Fig. 1 because the PA model cannot track both the primary- and secondary mode traverses in this region simultaneously.

Returning now to the form of the secondary-mode profile, let us begin to ask what interpretation should be made of it. The first thing to point out is that the primary- and secondary-mode profiles are not coincident in time. The two partial profiles have virtually identical half widths (fwhm) at 4.1°, however, the secondary-mode one arrives earlier by about 1.5°. Then there is the question of the 'outriders'! The leading feature can be traced to the isolated 'patch' at about $-23°$ longitude and $-30°$ PA in Fig. 1b which we pointed out earlier. The trailing feature is more difficult to see as it is below and to the right of – but immediately adjacent to – the principle primary-mode 'patch' at -9 to $-14°$ longitude and $\leqslant 90°$ PA. Note the asymmetry of the primary-mode feature, and the additional emission to the bottom right of it. Note also that the minimum between the 'MP' and the trailing feature in the secondary-mode partial profile falls just after $-7.5°$ longitude—and that there is a slight 'cusp' in the density distribution in Fig. 1b which apparently corresponds to it. Here the PA model used in the mode separation is sensitive to the position of the modal boundary, so that it effectively discriminates between the above primary-mode 'patch' and the secondary-mode power immediately adjacent to it. This criticality stems from the close separation in angle of the two modes in this region.

Readers may also question whether the secondary-mode features are in some manner generated by the mode-separation procedure. After all, most of the samples (86.0%) and a significant amount of the power (14.4%) in the original pulse sequence are not represented in Figs. 4(a and b) and accrue to the residual profile in Fig. 4c. In order to explore this possibility, partial profiles were computed holding the model PA parameters constant, but progressively reducing the noise threshold from 2σ to 1σ, 0σ, and even -1σ. Eventually, with the latter, the noise threshold becomes moot and all samples accrue to either one or the other modal partial profiles. The meaningless division of ever more noise-dominated samples into one or the other 'modal profiles' produces statistical travesties (total linear polarization $L > I$), but the form, boundaries, and relative amplitudes of the secondary-mode 'MP' and its 'outriders' remain intact. Therefore, we cannot trace their origin to an artefact of the partial-profile construction process. If there is an error, it must be in the interpretation of the primary- and secondary-mode related 'patches' in Fig. 1.

Turning now to the more recent 1992 observations, we see a very similar story overall. The pulsar appears to have been about 4 times weaker on the latter occasion, but 5 times the bandwidth and much better receivers were also being used in 1992. It is worth returning to Fig. 1 and again carefully comparing the two 430-MHz observations. The

MP in the 1992 observation is significantly narrower than that in the earlier one (3.7° versus 4.5°), owing perhaps to improved resolution. This seems to accentuate the asymmetry of L within the overall I envelope, and probably accounts in part for its larger relative amplitude as well. Very different, however, is the circular polarization; while the 1974 observation shows a small amount ($<5\%$) which varies antisymmetrically across the MP, the 1992 profile has nearly 15% RCP with only a hint of a sense reversal.

The primary-mode, secondary-mode, and residual partial profiles are given in Figs. 5(a–c), respectively. Little needs be said about the former except to note its narrowness (now about 3.2° fwhm), its increased linear symmetry as compared with the total profile, its nearly identical circular polarization, and of course its more orderly PA

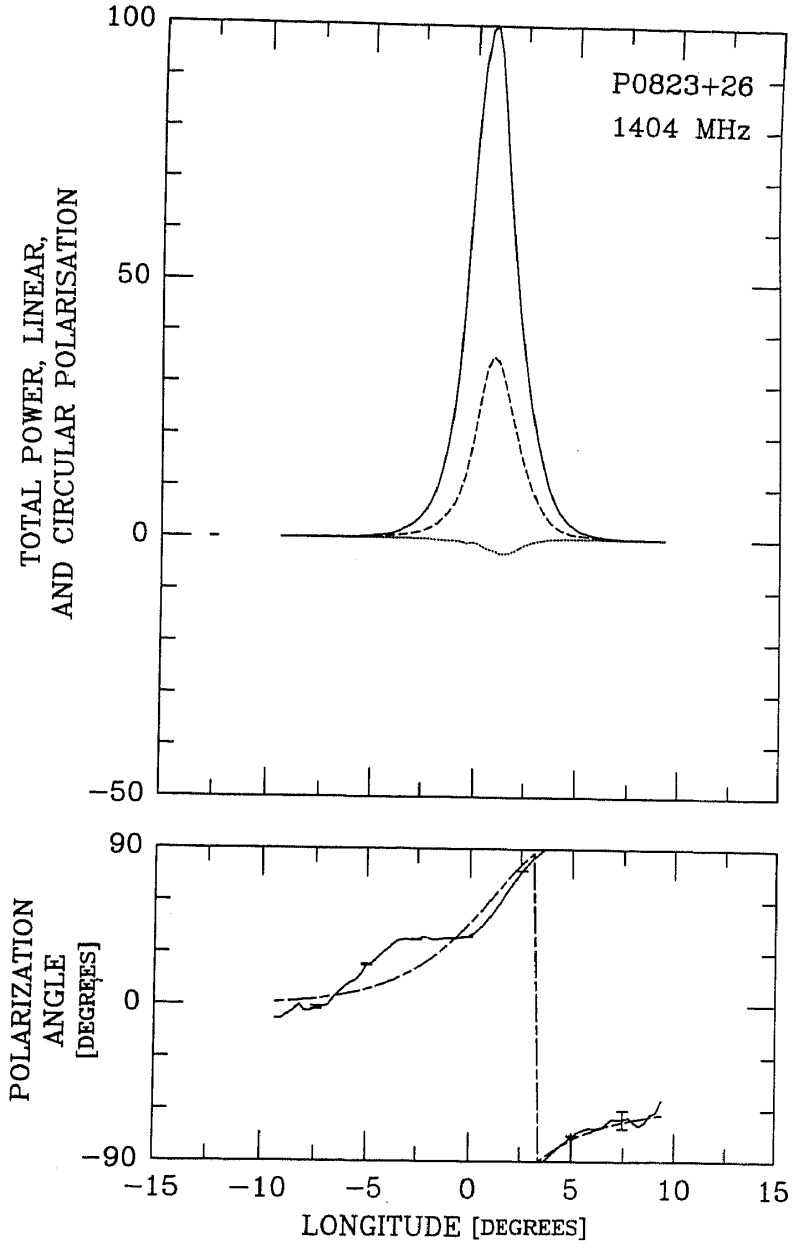

Figure 6(a).

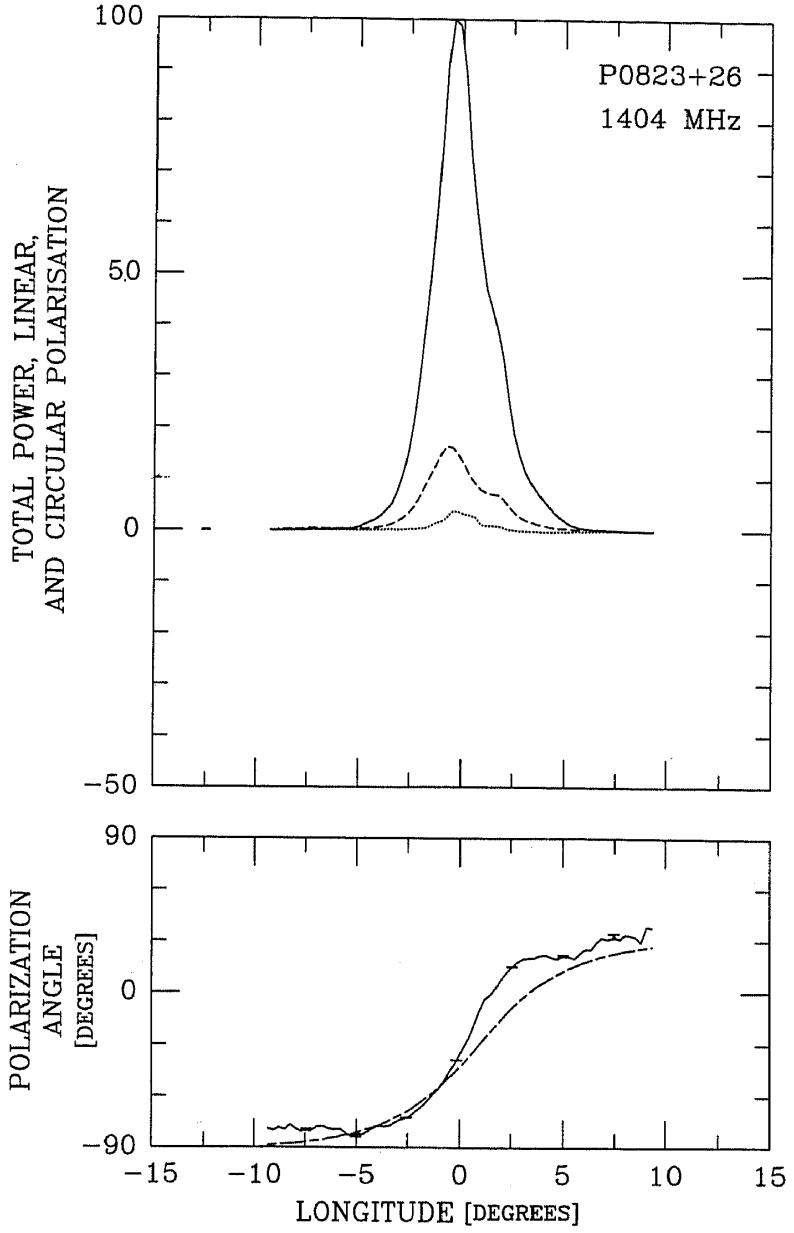

Figure 6(b).

traverse. With a 2-σ threshold, it here represents 10.1% of the samples and 68.9% of the total power in the individual-pulse sequence.

The secondary-mode profile in Fig. 5(b) again has a tripartite form, both in I and in total linear, L—although the minimum between the middle and trailing features is less well resolved. The fractional linear polarization seems to be a little larger than in the earlier observation. However, please note that the secondary-mode circular is very comparable, notwithstanding the very different primary-mode circular (again suggesting that a 'mode-changing' phenomenon is active in the pulsar which changes, over time, the relative proportions of the two polarization modes or their overall polarization states). The fwhm of the 'MP' is here about 3.3°, and it again leads the primary-mode one by almost exactly 1.5°. Here the secondary-mode

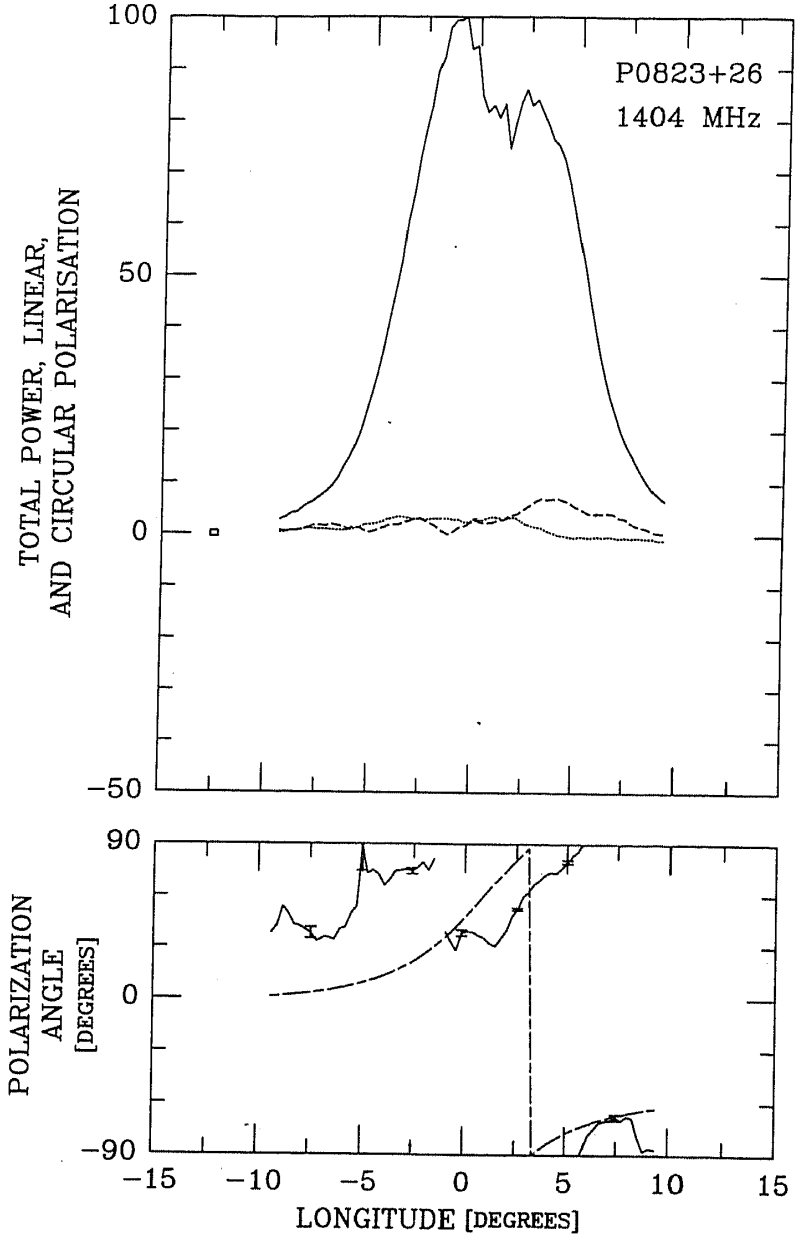

Figure 6(c).

Figure 6(a–c). Partial, 'mode-separated' profiles for pulsar 0823 + 26 at 1404-MHz on 9th October 1981 as in Fig. 4.

profile represents 4.0% of the samples and 19.0% of the power of the total individual-pulse sequence at an L-threshold value of 2σ. And, again, lowering the L threshold to irrelevance produces no qualitative change in the form of the secondary-mode profile.

'Mode-separated' profiles corresponding to the 1404-MHz observation in Fig. 1(c) are given in Figs. 6(a–c). Only a limited longitude range around the MP was available in these observations. The PA-model parameters used were similar to those given above. At this frequency 60.1% (16.5%) and 24.1% (8.4%) of the power (samples) accrued to the primary (Fig. 6a) and secondary (Fig. 6b) modes, respectively, and 15.8% (75.1%) to the residual (Fig. 6c) profile.

5. Main-pulse emission geometry

Rather few 'mode-separated' partial profiles, computed from well resolved and calibrated observations, are available in the literature; it is thus far too early to attempt any generalizations regarding them. In particular, the question of what constitutes a 'component' in total-average profiles has been a subject fraught with controversy (and is perhaps only now beginning to clarify); therefore we certainly have no wish to hastily attribute this status to every discernible minor feature in mode-separated partial profiles. Nevertheless, the appearance of the additional features in pulsar 0823 + 26's secondary-mode profile is so extraordinary that we are emboldened to attempt some speculative analysis.

Therefore, let us proceed by entertaining the hypothesis that the two new, minor features on the leading and trailing edges of the main one are indeed correctly interpreted as a conal-component pair, which was too weak to detect in the total profile at any frequency. We noted above—and reiterate here – that 0823 + 26, though almost certainly correctly classified as a core-single (S_t) pulsar, produces no identifiable conal 'outriders' even at the highest frequencies of observation. Thus, were we to interpret the secondary-mode features as 'outriders', we would encounter no conflict with our existing knowledge of this star.

A way to assess whether this interpretation makes sense is that of exploring its geometrical consequences. The basic magnetic geometry of this pulsar seems well established: Paper IV argued that core-component widths can be used to determine the latitude of the magnetic axis α, and pulsar 0823 + 26 was discussed not only as an example of a pulsar whose interpolated 1-GHz core width implies that $\alpha \simeq 90°$, but one whose overall PA traverse supports this, and whose interpulse (0823 + 26 is almost certainly a two-pole interpulsar) leaves virtually no doubt.

More questionable then is its emission geometry in relation to our sightline. Referring again to Fig. 1, recall that the maximum PA sweep rate R is about + 15°/° for the primary mode and about + 30°/° for the secondary one. Using the definition of R following equation (1), we see that this results in β values of + 3.8° and + 1.9°, respectively, where the '+' sign has been added to indicate that these are outside (positive) traverses on the basis of their flattened wings (see Narayan & Vivekanand 1982).

The significance of the β value associated with the primary mode is not yet clear, but we are immediately at liberty to use the secondary-mode β value, along with α and the (outside, half-power) width of the conal component pair to calculate the conal emission radius which would be expected. This latter value, scaled from the older and newer secondary-mode profiles in Figs. 4 and 5 are 16.7° and 16.3°, respectively. Now using equation (4) of Rankin (1993a; hereafter Paper VIa), this implies a conal radius ρ of just less than 8.5° (if we 'round' down to 16° in an effort to 'extrapolate' to 1 GHz, ρ is 8.2°; please see Rankin (1993b); hereafter Paper VIb, Table 4). In either case, 0823 + 26's secondary-mode ρ value is clearly just what one would expect for an outer cone, as can be seen by referring to equation (5) of Paper VIa.

It would then seem that the most economical interpretation of the 'outriders' in the secondary-mode profile of pulsar 0823 + 26 is that they indeed represent an outside conal component pair, which is so weak that it can be detected only by removing the dominant primary-mode power from the profile. This line of interpretation is entirely consistent quantitatively with the known geometry of the pulsar and further an answer to the question – for 0823 + 26, certainly, but also in general – of why some core-single pulsars have no discernible conal outriders.

6. Postcursor emission geometry

First, several different lines of argument now give similar conclusions regarding the basic geometry of pulsar 0823 + 26. Its interpulse (Hankins & Fowler 1986; Paper IV), analysis of its PA traverse (Lyne & Manchester 1988; Blaskiewicz *et al.* 1991), and the width of its MP core component (Paper IV) all indicate that its magnetic axis is nearly orthogonal to its rotational axis. Moreover, two somewhat different analyses, Lyne & Manchester (see especially, their table 2) and that in both this paper and Paper VIb, find that our sight line passes within a mere 1 or 2° of the magnetic axis.

Second, the identification above of the secondary-mode 'outriders' as an outer conal component pair marks these components as falling at the extreme boundary of conal emission in this pulsar, in terms both of angle from the magnetic axis and of distance from the star. We now have overwhelming evidence that conal emission is highly consistent in its angular beaming properties (Paper VIa & b; Gil *et al.* 1993; Gil & Kijak 1993); the outer conal emission radius is $5.75° P^{-1/2}$, or, as we saw in the previous section, about 8°.

In this geometric context it is now much more interesting to consider the significance of the postcursor component in pulsar 0823 + 26, and the first point to make is that we now have no possible option of viewing the PC component as some kind of weak, widely separated portion of a conal double profile as was attempted in Paper III. The PC lies much too far from the magnetic axis – some 30° – for it to be of conal origin in any usual sense; furthermore, there is *only* a PC, no precursor!

While we cannot say how it is that the PC is emitted, it would seem that 0823 + 26's geometry offers a particularly good opportunity to identify unusual types of emission. As noted above, not only is this pulsar's magnetic moment nearly parallel to its equator, but so is our sight line! Only in this geometry is there a bundle of field lines (also parallel to the star's rotational equator) which remains in view as the star rotates and has tangent points in the observer's direction for an unusually large fraction of the star's rotation period. One such bundle trails the magnetic axis, and it is worth noting that any 'field-line sweepback' at high altitude will increase the curvature of this bundle. Another bundle leads the magnetic axis, and (with enough sweepback) it could also have tangents in the observer's direction, but only at great altitude and for a shorter interval.

If the PC component is emitted along this trailing bundle of peripheral, equatorial field lines at a height at which the field remains essentially dipolar, then it is possible to estimate the emission height of the PC, again using equation (2) in Paper VIa. For an angular separation between the PC and the magnetic axis (taken to be the MP peak) of about 32° (Hankins & Fowler 1986), we find an emission height of about 4×10^3 km – that is, about 400 stellar radii or some 4% of the light-cylinder radius – as compared to the nominal 210-km emission height of the outer cone. Any poloidal distortion of the field would increase the curvature of the trailing bundle of equatorial field lines and decrease the emission height. Interestingly, it would also decrease that of the leading bundle, perhaps explaining why we more generally see postcursors rather than precursors. Both height and sweepback will tend to increase the curvature of the trailing bundle, which may favour emission by particles with quite different energies than those responsible for the MP. Theories of pair-production discharge above pulsar polar caps, seem to produce a broad distribution of particle energies (Daugherty and Harding 1986). Finally, we note that the MP-PC separation *increases*

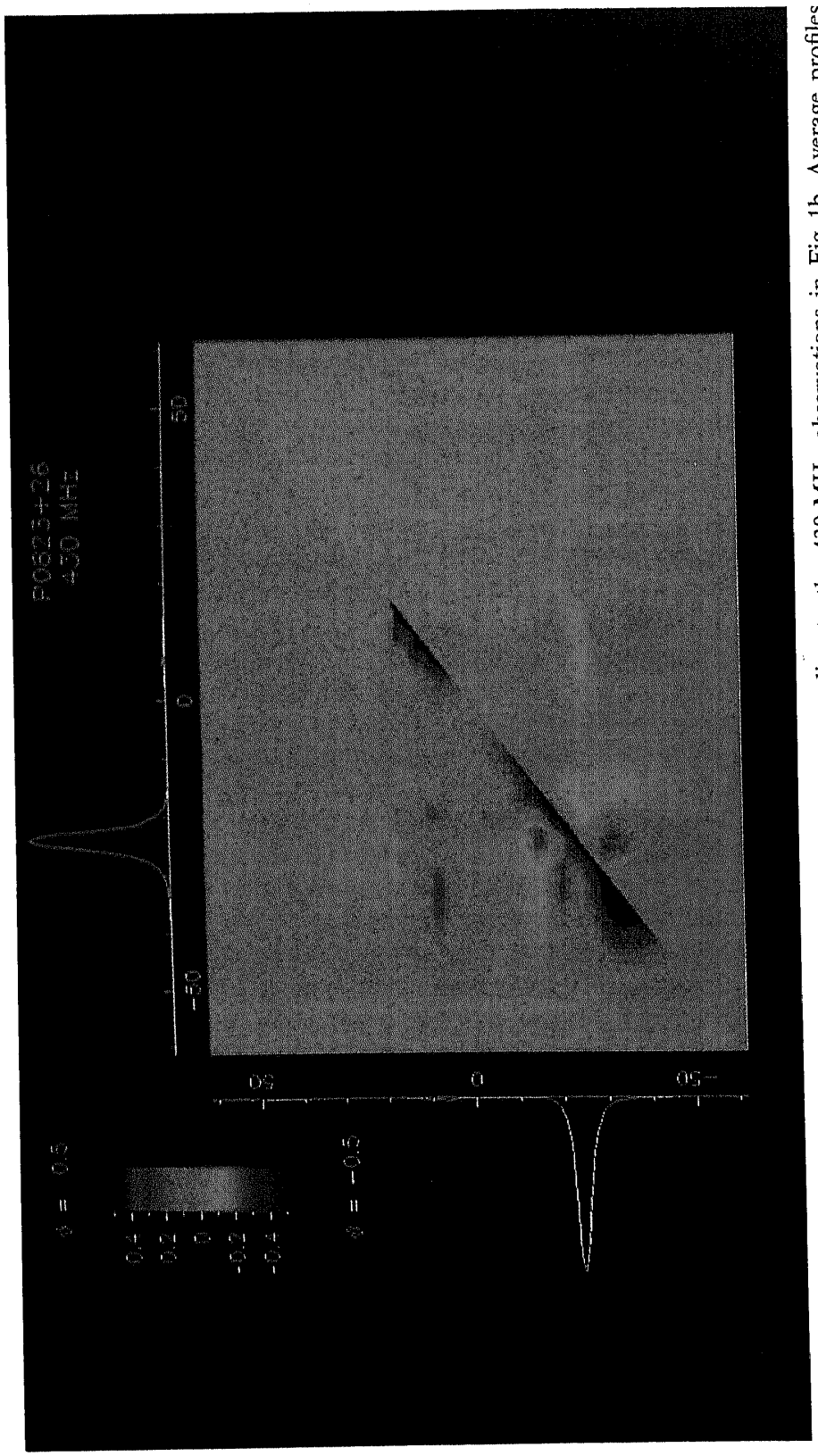

Figure 7. Longitude-to-longitude intensity correlation plot corresponding to the 430-MHz observations in Fig. 1b. Average profiles comprising the noise, the MP-PC, and IP windows have been plotted on both axes for convenience, and at longitudes larger than $-15°$ the quantities I, L and V have been multiplied by a factor of 5 to show the postcursor and interpulse regions more clearly. The correlation is indicated by a coloured rectangle at the intersection of the two longitudes, and the colour scale in the upper left hand corner of the figure gives the magnitude of the correlation coefficient. The figure is divided into two triangular regions, the upper left one (row number > column number), gives the correlation of the current pulse with itself at different longitudes (zero lag); whereas, the lower right one gives the correlation between the current pulse and the previous pulse (lag = -1).

weakly with frequency, suggesting that the higher frequency PC emission is emitted at greater heights than the low frequency emission; if so, this would be a 'radius-to-frequency mapping' of the opposite sense to that usually encountered.

If this is the correct interpretation for the geometry of the PC component, then we note that both the PC and the latter conal outrider are emitted along the same bundle of trailing equatorial field lines. It is then possible that the two components will exhibit some correlation in the intensities of their constituent individual pulses. The longitude-to-longitude correlation of the total power, corresponding to the 430-MHz observations in Fig. 1b, is given in Fig. 7. The longitude, of course, labels both axes, and average profiles comprising the noise, the MP-PC, and IP windows have been plotted for convenience. A colour scale indicating the degree of correlation is given at the upper left of the figure. The upper triangular region shows that the longitude-longitude correlations are calculated by correlating the emission in the same pulse at different longitudes (zero lag). In the lower triangular region, the emission at any given longitude corresponding to the row number is correlated with emission in the previous pulse at longitude corresponding to the column number (lag = + 1). The diagonal line is included in the lower part with lag = + 1.

This figure clearly shows the correlation between the MP and PC emission. Interestingly, the correlation is significant only between the central portion of the PC and the wings of the MP; between the center of the MP and the PC there is hardly any significant correlation. If anything, the emission in the center of the MP is anti-correlated with the PC emission of the previous pulse, as can be seen from the lower part of the figure. However, the correlation between the wings of the MP and PC persists even for a one-period lag. Similarly, the MP leading and trailing wings exhibit highly correlated emission, but this emission is not significantly correlated with that of the MP center. Another curious feature is the anti-correlation between the MP peak and the 'bridge' region between the MP and PC. This correlation was also noted by Popov & Sieber (1990) in their 1700-MHz study, although their observations were restricted narrowly to the MP region. There is also a significant correlation between the leading part of the previous MP and the current IP peak.

All this notwithstanding, we note that there are five other pulsars with known PC components: The Crab pulsar is usually discussed as having a 'precursor' component, but in that this component appears to be a core component (Paper IV), one might better regard the star's MP as a postcursor to it. Then there are 0940 + 16, 1530 + 27 (Rankin *et al.* 1989), probably 1530 − 53 (McCulloch *et al.* 1978; Manchester *et al.* 1980; McCulloch *et al.* 1982), 1929 + 10 (Perry & Lyne 1985; Rankin & Rathnasree 1996), and more recently 2217 + 47 (Suleymanova & Shitov 1994). We know of no pulsar with a true precursor – that is, one with a weak patch of emission which leads a core component. Apart from the Crab pulsar and 1929 + 10 – which are almost certainly orthogonal rotators – we know very little about the geometry of these other stars; most have not even been adequately classified, in part because of their odd 'postcursor' emission. Somewhat more is known about 2217 + 47; it was classified as an S_t pulsar in Paper VIb with an α of only 42°. This value could easily increase, however, as the profiles available in the literature are mostly poor (the only ~ 400-MHz profile available is from LSG in 1971!) and thus probably not well resolved.

We note that pulsars 0823 + 26 and 2217 + 47 have very similar periods and period derivatives, and the completely equatorial model used above to discuss the emission

geometry of the former also provides an attractive scenario for understanding Suleymanova & Shitov's observations of the latter. Perhaps the most surprising feature of the 2217 + 47 postcursor is that it slowly varied in amplitude and position over time, possibly correlated with changes in the torque on the star. Indeed, if the PC emission is occurring high on this bundle of trailing, equatorial field lines, torque changes might change the curvature and thus the height of the radiation, which would in turn change its phase within the profile relative to the core component. But we do not yet know whether 2217 + 47 – or really any of the other 'postcursor' pulsars apart from the Crab – have orthogonal geometries. We are guessing that they probably do, but additional observations and analysis are required to answer this question. If so, some – 2217 + 47 to be sure – may prove highly useful as a means of exploring other regions of the pulsar magnetosphere. Pulsars with PC components may also be good candidates in which to search for new interpulses.

7. Interpulse emission geometry

Little can be said with confidence about pulsar 0823 + 26's interpulse geometry. No quality observation of this feature exists in the literature, and, given its weakness, none may be possible in the foreseeable future. Nonetheless, the 430-MHz profile (Rankin & Benson 1981) appears more single, and the 1400-MHz profile (Rankin *et al.* 1989) has a flat top which might indicate incipient conal outriders (as per the usual triple or possibly conal-single evolution). Both IP profiles have a full width at half maximum of about 16 or 17°, and the PA sweep rate is about $-6°/°$. These values do not make any immediate sense in terms of the geometrical arguments of Paper VIa & b. If the above width corresponds to an outer cone, either the IP sweep rate needs to be steeper or the width smaller. One possibility is that here we are cutting an outer cone on its extreme edge, so that the sightline comes nowhere near the high-intensity 'shoulder' of the conal beam.

8. Polarization-modal structure of PSR 0823 + 26's emission

We have seen above that the primary mode at 430 MHz represents about 68–69% and the secondary-mode about 18–19% of the total power in the sequence of pulses when the threshold is set at a level such that L must exceed about two σ in the off-pulse noise; that is, the primary mode is about 3.5 times stronger than the secondary one. Of course, these numbers will change somewhat if **a**) the mode-separation algorithm is not accurately segregating the modal power in the PA-longitude diagram, **b**) if the L threshold level is changed, or **c**) if the emitted modal power varies in time. We have done our best to assure that the modal separation is correct, although given the proximity of the two modes near the primary-mode 'blotch' in Fig. 1, some ambiguity is unavoidable. As for the second condition, a 2-σ threshold gives a sample uncertainty in the PA of $\pm$ 30°, and any lower threshold will increase the number of unpolarized or noise-dominated samples which are spuriously assigned to one mode or the other. We re-emphasize that only for those samples with adequate residual linear polarization can we make a choice about their mode. For the others, all such information has been lost through depolarization on time scales short compared to the sampling interval, and we

can only speculate about the significance of this depolarized portion of the pulsar's emission. Observations suggest either that these are relatively stable or that we have found the pulsar in the same 'modal' state.

We can then ask whether this is the 'true' power ratio of the two modes. Some 12–14% of the power fell below the threshold in L, and the average of these 'residual' samples shows virtually no linear polarization. It might then be **a**) that most of this power is associated with the secondary mode, which is only some 10% polarized, in which case the modal ratio is about 70/30%, **b**) that the power is about equally divided between the two modes (and, indeed, the residual PA falls near the primary mode before the MP peak and near the secondary mode thereafter) in which case the modal ratio is about 75/25%, or **c**) that most of the residual power is associated with the primary mode in view of its greater intensity, in which case the modal ratios are about 80/20%. At 21 cm about 60% of the power was found in the primary mode to about 24% and 16% for the secondary mode and residual categories; see Fig. 6. If the polarization-mode switching phenomenon is broad band – as, indeed, it appears to be – these latter numbers might be squared with any of the three alternatives.

It is also useful to consider the fractional linear polarization, and comparing the total average profiles in Fig. 1 with the modal partial profiles in Figs. 4–6 we see that the mode separation did not dramatically increase the fractional linear polarization, either at 430 or 1400 MHz. The earlier 430-MHz observation has a peak fractional linear polarization of about 35%, whereas the primary mode's is only about 42%. Similarly, that of the later 430-MHz run goes from about 45% to 52% and the 1400-MHz one from about 28% to 36%. The later data are better resolved than the earlier at both 430 and 1404 MHz, and this may be responsible, in part, for their somewhat larger amounts of aggregate linear polarization.

In all cases the secondary-mode fractional linear is lower. We then apparently have a situation in pulsar 0823 + 26 wherein very significant amounts of depolarization are occurring on time scales shorter than the inherent time resolution of the observations – here in all cases some part of 1° longitude. This also largely explains the fact that the secondary mode is more depolarized than the primary one, because secondary-mode samples will typically contain more primary-mode power than primary ones will secondary-mode power, by simple reason of their relative intensities. Only those unusual samples in which the secondary mode dominates the primary will be recognized as 'secondary-mode' samples—and accumulate in the 'secondary-mode' profile. Generally the secondary mode will just exceed the primary, and these are the conditions which are most depolarizing. These factors are especially complicated in 0823 + 26, however, owing to the spectacular non-orthogonality of the two modes throughout the duration of the MP.

9. Displaced modal emission in the main pulse

A very interesting feature of the modal partial profiles in Figs. 4–6 is the displacement in phase between the primary and secondary modes. Reference to these figures shows that the secondary mode 'MP' always leads the primary-mode feature, at 430 MHz by $1.5 \pm 0.1°$ and at 1404 MHz by some $1.3 \pm 0.1°$. Displacement in rotational phase has been seen before in the components of mode-separated profiles – the first component of

1737 + 13, for instance, shows a dramatic offset (Rankin *et al.* 1988) – however, this effect has not, before to our knowledge, been identified in a core component[@].

The question is what interpretation to make of this phase delay, and at this point two possibilities seem open. The first is that the offset is a geometrical phenomenon. We saw above that the observed offset was somewhat greater at 430 as compared to 1400 MHz – but just so within the errors – and just over 1° of longitude is quite comparable to the 3.36° diameter of the pulsar's polar cap. Another possibility is that we are here seeing an effect of birefringent propagation in the pulsar's inner magnetosphere as suggested, for instance, by Barnard & Arons (1986). If this is the case we might expect the effect to become more pronounced at lower frequencies—and furthermore this 'double' nature of the core component might be connected with such well known, but entirely unexplained phenomena such as 'absorption' and the observed broadening of some core components at lower frequencies (see Paper II).

10. Summary and conclusions

The polarization structure of the radiation which comprises pulsar 0823 + 26's average profile at both 430 and 1400 MHz has been studied. Two polarization modes are identified in the emission over a substantial range of longitudes around the MP and PC. In some intervals they are roughly orthogonal; however, just under the MP the two modes are more conspicuously non-orthogonal – and thus difficult to distinguish – than in any other pulsar we know of. We have attempted to construct partial profiles in which the power in the two polarization modes is largely separated and have identified two (mostly) continuous, non-orthogonal PA trajectories which seem to correspond to these modes. The primary mode in 0823 + 26 is three to perhaps five times stronger than the secondary mode overall and thus dominates the emission and the PA at most longitudes. It is then not surprising that the primary-mode MP closely resembles the total-profile MP.

The secondary-mode profile consists of three MP features, which appear to be a central core component and a surrounding pair of conal outriders. The (outside half-power) width of the outriders together with the secondary-mode PA traverse appear compatible with the interpretation that these conal features represent an outer emission cone.

This technique could lead to the discovery of covert emission features in the profiles of other pulsars with single profiles but complicated PA histograms. In this context, it is interesting to speculate about the emission geometry of the PC feature, which follows the MP by some 30°. Having now identified a pair of much more closely spaced components, which appear to represent an outer cone of emission, it is clear that the PC cannot be a conal component in any usual sense.

Overall, 0823 + 26 seems to have a nearly equatorial geometry—that is, both the magnetic axis and the sight line appear to lie close to the rotational equator of this pulsar. We then note that in this situation there is a bundle of trailing field lines which has a tangent in our direction for a substantial portion of the rotation cycle of the

[@] Pulsar 1737 + 13's core component is also misaligned in the mode-separated profiles, but given the greater complexity of both partial profiles, it is not at all clear what interpretation to make of this circumstance.

pulsar. Perhaps it is emission along this bundle – at a height of some 4×10^3 km or about 4% of the light cylinder – that the PC emission occurs.

If the PC component and the trailing conal outrider are both emitted along this trailing bundle of equatorial field lines, then it is possible that their emission is correlated. Indeed, we find that there is significant correlation between the PC and the longitude ranges of the trailing conal outriders, and furthermore that this correlation becomes negligible between the PC and the core-emission region.

Finally, it seems that the pulsar does exhibit some $6.4 \pm 0.8\%$ null pulses, which is somewhat more than the 5% limit of Ritchings (1976).

Acknowledgements

We thank Amy Carlow, Vera Izvekova, Svetlana Suleymanova, and Kyriaki Xilouris for help with the October 1992 observing and Dan Stinebring for making the Arecibo P-467 observations available. We also acknowledge Mark McKinnon for helpful discussions. One of us (JMR) also wishes to acknowledge the support of the U.S. Educational Foundation in India and the hospitality of the Raman Research Institute, where part of this work was carried out while she was in residence on a Fulbright Fellowship. This work was supported in part by a grant from the U.S. National Science Foundation (AST 89-17722). Arecibo Observatory is operated by Cornell University under contract to the U.S. National Science Foundation.

References

Backer, D. C., Boriakoff, V., Manchester, R. N. 1973, *Nat. Phys. Sci.*, **243**, 77.
Backer, D. C. 1973, *Astrophys. J.*, **182**, 245.
Backer, D. C., Rankin, J. M. 1980, *Astrophys. J. Suppl.*, **42**, 143.
Barnard, J. J., Arons, J. 1986, *Astrophys. J.*, **302**, 138.
Bartel, N., Sieber, W., Wielebinski, R. 1978, *A & A.*, **68**, 361.
Blaskiewicz, M., Cordes, J. M., Wasserman, I. 1991, *Astrophys. J.*, **370**, 643.
Cordes, J. M., Rankin, J. M., Backer, D. C. 1978, *Astrophys. J.*, **223**, 961.
Craft, H. D., Lovelace, R. V. E., Sutton, J. M. 1968, *I. A. U. Circ. No. 2100.*
Daugherty, J. K., Harding, A. K. 1986, *Astrophys. J.*, **309**, 362.
Gil, J. A., Snakowski, J. K., Stinebring, D. R. 1991, *Astrophys. J.*, **242**, 119.
Gil, J. A., Lyne, A. G., Rankin, J. M., Snakowski, J. K., Stinebring, D. R. 1992, *A&A*, **255**, 181.
Gil, J. A., Kijak, J. 1993, *A & A*, **273**, 563.
Gil, J. A., Kijak, J., Seiradakis, J. H. 1993, *A&A*, **272**, 268.
Hagan, J. 1987, *NAIC Electronics Department Manual No. 8319.*
Hankins, T. H., Fowler, L. A. 1986, *Astrophys. J.*, **304**, 256.
Hankins, T. H., Rickett, B. J. 1986, *Astrophys. J.*, **311**, 684.
Hankins, T. H., Rankin, J. M. 1994, private communication.
Izvekova, V. A., Kuz'min, A. D., Malofeev, V. M., Shitov, Yu. P. 1981, *Astrophys. Space Sci.*, **78**, 45.
Komesaroff, M. M. 1970, *Nature*, **225**, 612.
Kramer, M., Wielebinski, R., Gil, J. A., Seiradakis, J. H., Jessner, A. 1994, *A&A*, **107**, 527.
Lang, K. R. 1969, *Astrophys. J. Lett.*, **158**, L175.
Lyne, A. G., Manchester, R. N. 1988, *Mon. Not. R. astr. Soc.*, **234**, 477.
Manchester, R. N., Hamilton, P. A., McCulloch, P. M. 1980, *Mon. Not. R. astr. Soc.*, **192**, 153.
McCulloch, P. M., Hamilton, P. A., Manchester, R. N., Ables, J. G. 1978, *Mon. Not. R. astr. Soc.*, **183**, 645.
McCulloch, P. M., Hamilton, P. A., Manchester, R. N. 1982, private communication.

Narayan, R., Vivekanand, M. 1982, *A&A*, **113**, L3.
Perillat, P. 1988, *NAIC Computer Department Report # 23.*
Perillat, P. 1992, private communication.
Perry, T. E., Lyne, A. G. 1985, *Mon. Not. R. astr. Soc.*, **212**, 489.
Phillips, J. A., Wolszczan, A. 1992, *Astrophys. J.*, **385**, 273.
Popov, M. V., Sieber, W. 1990, *Sov. Astr.*, **34**, 382.
Radhakrishnan, V., Cooke, D. J. 1969, *Astrophys. J. Lett.*, **3**, 225.
Rankin, J. M. 1983b, *Astrophys. J.*, **274**, 359. (Paper II)
Rankin, J. M. 1986, *Astrophys. J.*, **301**, 901. (Paper III)
Rankin, J. M. 1988, *Astrophys. J.*, **325**, 314.
Rankin, J. M. 1990, *Astrophys. J.*, **352**, 247. (Paper IV)
Rankin, J. M. 1993a, *Astrophys. J.*, **405**, 285. (Paper VIa)
Rankin, J. M. 1993b, *Astrophys. J.* (*Suppl.*), **85**, 145. (Paper VIb)
Rankin, J. M., Benson, J. M. 1981, *Astr. J.*, **86**, 418.
Rankin, J. M., Campbell, D. B., Backer, D. C. 1974, *Astrophys. J.*, **188**, 609.
Rankin, J. M., Campbell, D. B., Spangler, S. 1975, *NAIC Report # 46.*
Rankin, J. M., Rathnasree, N. 1996, in preparation.
Rankin, J. M., Stinebring, D. R., Weisberg, J. M. 1989, *Astrophys. J.*, **346**, 869.
Rankin, J. M., Wolszczan, A., Stinebring, D. R. 1988, *Astrophys. J.*, **324**, 1048.
Ritchings, R. T. 1976, *Mon. Not. R. astr. Soc.*, **176**, 249.
Sieber, W. 1973, *A&A*, **28**, 237.
Stinebring, D. R., Cordes, J. M., Rankin, J. M., Weisberg, J. M., Boriakoff, V. 1984, *Astrophys. J.* (*Suppl.*), **55**, 247.
Suleymanova, S. A., Shitov, Yu. P. 1994, *Astrophys. J. Lett.*, **422**, L17.
Taylor, J. H., Huguenin, G. R. 1969, Symposium on Pulsars and High Energy Activity in Supernova Remnants, Academia Nationale dei Lincei, Rome, 1969 December 18.
Xilouris, K. M., Seiradakis, J. M., Gil. J., Sieber, W., Wielebinski, R. 1995 *A&A*, **293**, 153.